

Model of Electrochemical “Double Layer” Using the Phase Field Method

J. E. Guyer^{*}, W. J. Boettinger, J. A. Warren

Metallurgy Division

G. B. McFadden

Mathematical and Computational Sciences Division

National Institute of Standards and Technology, Gaithersburg, MD 20899, USA

Abstract

We present the first application of phase field modeling to electrochemistry. A free energy functional that includes the electrostatic effect of charged particles leads to rich interactions between concentration, electrostatic potential, and phase stability. The present model, explored for the equilibrium planar interface, properly predicts the charge separation associated with the equilibrium double layer at the electrochemical interface and its extent in the electrolyte as a function of electrolyte concentration, as well as the form expected of surface energy vs. potential (“electrocapillary”) curves.

1 Introduction

The phase field technique has previously been applied to the time evolution of complex dendritic, eutectic, and peritectic solidification morphologies [1,2]. The present work was motivated by the mathematical analogy between the governing equations of solidification dynamics and electroplating dynamics. For example, the solid-liquid interface is analogous to the electrode-electrolyte interface. The various overpotentials of electrochemistry have analogies with the supercoolings of alloy solidification: diffusional (constitutional), curvature, and interface attachment. Dendrites can form during solidification and during

^{*} Corresponding author.

Email address: guyer@nist.gov (J. E. Guyer).

electroplating. Nonetheless, we find significant differences between the two systems.

Electrochemistry has been chosen by the microelectronics industry as the deposition method for “copper damascene” interconnects on microchips because it is capable of filling trenches and vias [3,4] without “pinch-off” void formation problems associated with chemical or physical vapor deposition. Because plating into such small features naturally involves large curvatures of the growing interface and large electric field gradients, a rigorous mathematical solution of the governing equations is warranted.

Modeling the evolution of a sharp interface, particularly when the topology is changing during growth, is a challenging problem because the boundary conditions at that interface are dependent on the shape and location of the interface. The phase field method avoids these difficulties by introducing a new phase variable and an appropriate governing equation for that variable. The governing equations for the system can then be solved on a uniform grid, with the interface position as one of the results of the solution. A simple analytical electrochemical cell consists of a working electrode, an electrolyte, and a reference electrode. In the case of electroplating, there will also be a counter electrode. The phase field variable in this work describes the transition between the working electrode and the electrolyte.

1.1 Length scales in electrochemistry

There are three significant length scales in electrochemistry:

- (1) the thickness of the electrode-electrolyte interface,
- (2) the charge separation (of the capacitive double layer) and voltage decay distance, which are related to the concentrations of charged species and the dielectric constant,
- (3) and the long range concentration decay length due to diffusion and convection in the electrolyte (related to the ratio of diffusivity to interfacial velocity).

In traditional modeling of the equilibrium electrochemical interface, the electrode-electrolyte interface is assumed to be sharp, as shown in Figure 1. The charge separation distance is considered diffuse in the electrolyte only, with any excess charge on the electrode residing entirely at the metal surface. In the electrolyte, there may be some specific adsorption of ions on the interface, and a more diffuse distribution of ions further away. Some ions may be complexed with solvent molecules, giving them a larger effective size and limiting their approach to the electrode surface (we do not consider solvation in this work). The long range concentration decay length is absent for an equilibrium

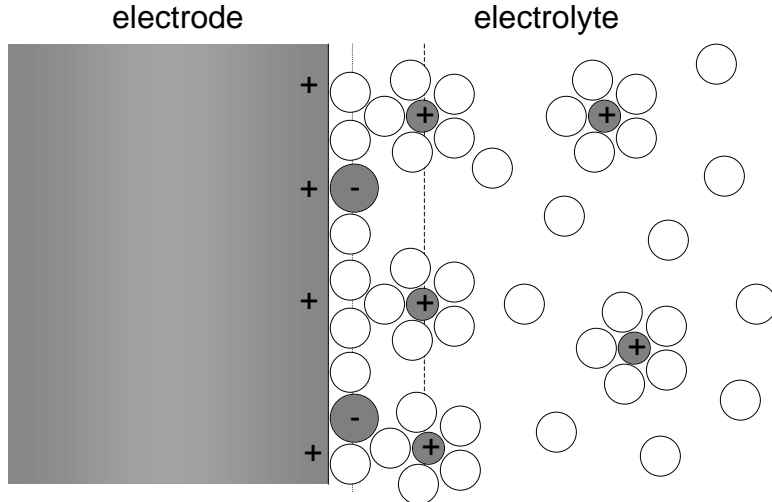


Fig. 1. Schematic of the electrode-electrolyte interface.

interface. This equilibrium regime is characteristic of models such as that of Gouy and Chapman. By requiring that the ions in solution must simultaneously satisfy a Boltzmann distribution and Poisson's equation, a description of the charge distribution is obtained, with predictions for the surface energy, charge separation, and adsorption.

In another limit of traditional modeling, primarily used for dynamics, the electrode-electrolyte interface is assumed sharp and the charge separation is a dipole layer. The long range concentration decay length is modeled by transport in a stagnant fluid boundary layer. In equilibrium, the concentration and electrostatic potential jump across the interface are related by the Nernst equation

$$\psi^{\text{eq}} = \psi^\circ + \frac{RT}{z\mathcal{F}} \ln \frac{C_O}{C_R} \quad (1)$$

where ψ^{eq} is the equilibrium electrostatic potential jump, ψ° is the standard potential, R is the molar gas constant, \mathcal{F} is Faraday's constant, T is the temperature, C_O is the concentration of the electroactive species in the oxidized state, C_R is the concentration in the reduced state, and z is the number of electrons transferred in the redox reaction. A term $-V_m\gamma K/z\mathcal{F}$ is added to the right hand side of Eq. (1) to treat curved interfaces, where V_m is the molar volume, γ is the surface energy, and K is the curvature. In dynamic conditions, a chemical reaction rate description (such as the Butler-Volmer relation) is used to describe the relationship between potential jump and current.

In the present phase field model, all three length scales are assumed to be important (albeit different) and all are modeled together with the same equations in the metal and electrolyte. This simplifies treatment of complex geometries

and permits proper treatment of adsorption and its effect on interface kinetics. As usual for phase field models, though, the equations can be very stiff, requiring significant computational resources.

1.2 Traditional double-layer theory (Gouy-Chapman)

The best known sharp-interface model of the electrochemical interface is that of Gouy and Chapman [5,6]. In this model (and its variants), the electrode is not considered, the distribution of ions in the electrolyte is assumed to follow a Boltzmann distribution

$$C_j = C_j^\infty \exp \left[\frac{-z_j \mathcal{F} (\psi - \psi_\infty)}{RT} \right] \quad (2)$$

and to satisfy Poisson's equation

$$\rho = \sum_N C_j z_j \mathcal{F} = -\epsilon \frac{d^2 \psi}{dx^2}. \quad (3)$$

C_j is the concentration of species j , C_j^∞ is the concentration of species j in the bulk electrolyte, z_j is the valence of species j , ρ is the charge density, ϵ is the permittivity of the electrolyte, and the electrostatic potential field $\psi = \psi_\infty$ in the far field. In a $z:z$ electrolyte (cation and anion have equal and opposite valence), these equations reduce to

$$\frac{d\psi}{dx} = - \left(\frac{8RT C^\infty}{\epsilon} \right)^{1/2} \sinh \left[\frac{z \mathcal{F} (\psi - \psi_\infty)}{2RT} \right], \quad (4)$$

which has the solution

$$\frac{\tanh [z \mathcal{F} (\psi - \psi_\infty) / 4RT]}{\tanh [z \mathcal{F} (\psi_0 - \psi_\infty) / 4RT]} = \exp (-x/l_\psi). \quad (5)$$

ψ_0 is the electrostatic potential in the electrolyte at the electrode surface ($x = 0$) and $l_\psi = [\epsilon RT / (2C^\infty z^2 \mathcal{F}^2)]^{1/2}$ is the voltage/concentration decay length (the same as the Debye length).

Using this model, the surface energy, surface charge, differential capacitance, adsorption and other interfacial parameters can be related to the voltage across the interface. The surface charge on the electrode σ^S is described by

$$\sigma^S = - \left(\frac{\partial \gamma}{\partial \psi_0} \right)_{\mu_i} \quad (6)$$

where γ is the surface energy, and subscript μ_i denotes that the partial derivative is taken at constant chemical potential, *i.e.*, at constant activities (or

concentrations) of all species, as approximated on an inert mercury electrode. A plot of surface energy as a function of ψ_0 is known as an “electrocapillary curve” and from Eq. (6) we see that its maximum corresponds to the so-called “potential of zero charge”, where there is no net surface charge on the electrode (and due to overall charge balance, none in the electrolyte).

2 Phase Field Model

2.1 Components

The phase field approach requires a set of equations that can describe the evolution of conditions at every point in the system. Thus we must identify the chemical components that describe the electrode and electrolyte simultaneously. As our model problem, we consider a Cu metal electrode in contact with a CuSO_4 aqueous electrolyte. We choose our electrode to be a solid solution of Cu^{+2} and interstitial e^- . We choose our electrolyte to be an aqueous solution of H_2O , Cu^{+2} , and SO_4^{-2} . We assume that the partial molar volume of e^- is zero and that the partial molar volumes of Cu^{+2} , H_2O , and SO_4^{-2} are all the same, such that

$$V_m = \sum^N \bar{V}_j X_j = \bar{V}_S \sum^S X_j \quad (7)$$

and

$$\sum^S C_j = \frac{1}{\bar{V}_S}, \quad (8)$$

where V_m is the molar volume, $X_j = C_j V_m$ is the mole fraction of component j with partial molar volume \bar{V}_j , N is the set of all components, and S is the set of substitutional components with partial molar volume \bar{V}_S . This treatment of e^- as interstitials allows the motion of e^- to decouple from the other species. The simplification that all substitutional species have the same, constant partial molar volume allows us to consider diffusion separately from deformation.

2.2 Free energy

The free energy of this two phase system of N charged species is given by

$$F(\varphi, C_1, \dots, C_N, \psi) = \int_V \left[f_V(\varphi, C_1, \dots, C_N) + \frac{1}{2} \rho \psi + \frac{\kappa_\varphi}{2} |\nabla \varphi|^2 \right] dV \quad (9)$$

where F is the total Helmholtz free energy, f_V is the Helmholtz free energy per unit volume, φ is the phase field variable, and κ_φ is the phase field gradient energy coefficient. $\varphi = 1$ denotes the electrode and $\varphi = 0$ denotes the electrolyte. The first term in the integral of Eq. (9) describes the chemical energy, the second term describes the electrostatic energy, and the third term describes the interfacial energy of the phase field.

2.3 Equilibrium

We compose a Lagrangian from Eq. (9) by requiring that mass of each species must be conserved, and that Poisson's equation (3) and the substitutional constraint Eq. (8) must be satisfied everywhere in the system. By taking the virtual variations of this Lagrangian, we find that the governing equations in equilibrium are

$$\bar{\mu}_j - \frac{\bar{V}_j}{V_S} \bar{\mu}_s = \text{constant}, \quad (10)$$

$$0 = \frac{\partial f_V}{\partial \varphi} - \kappa_\varphi \nabla^2 \varphi - \frac{\epsilon'(\varphi)}{2} (\nabla \psi)^2, \quad (11)$$

and Poisson's equation (3). The electrochemical potential of species j is

$$\bar{\mu}_j = \frac{\partial f_V}{\partial C_j} + \mathcal{F} z_j \psi. \quad (12)$$

The subscript s denotes the solvent, chosen arbitrarily from the set S . The complete derivation of these equations is given in Ref. [7].

2.4 Choice of thermodynamics

To simplify our model as much as possible, we choose to describe the chemical Helmholtz free energy by ideal solution thermodynamics

$$f_V(\varphi, C_j) = \sum_N C_j \left\{ \mu_j^{\circ L} + \Delta \mu_j^{\circ p}(\varphi) + RT \ln C_j V_m + W_j g(\varphi) \right\} \quad (13)$$

such that

$$\bar{\mu}_j = \mu_j^{\circ L} + \Delta \mu_j^{\circ p}(\varphi) + RT \ln C_j V_m + z_j \mathcal{F} \psi + W_j g(\varphi). \quad (14)$$

$\mu_j^{\circ L}$ is the standard chemical potential of component j in the electrolyte, $\Delta \mu_j^{\circ}$ is the difference between the standard chemical potentials of component j

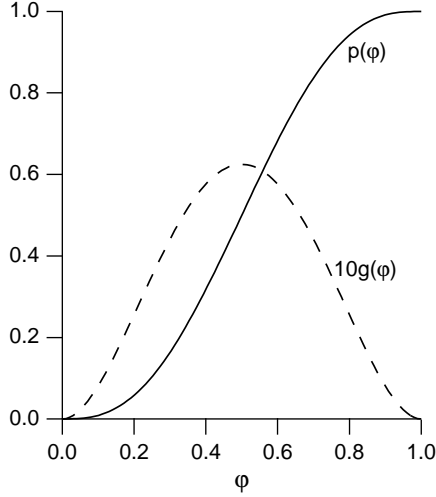


Fig. 2. Phase field double well and interpolation functions.

in the electrode and in the electrolyte, and W_j is the barrier height of the phase-field double well for component j . Other choices are possible, but we select

$$p(\varphi) = \varphi^3 (6\varphi^2 - 15\varphi + 10) \quad (15)$$

for the phase field interpolation function p , which is a smoothed step function, and

$$g(\varphi) = \varphi^2 (1 - \varphi)^2 \quad (16)$$

for the phase field double well function g . These functions are plotted in Figure 2.

2.5 Choice of parameters

If we consider only the values of concentration and potential far from an equilibrium interface ($\varphi = 0$, $\varphi = 1$), we can make contact with the sharp interface picture. Analysis of Eqs. (10) and (11) yields the fact that the far field values of the electrochemical potentials $\bar{\mu}_j$ are equal. From Eq. (14) (evaluated at $\varphi = 0$ and $\varphi = 1$), we see that, for all species,

$$\psi^S - \psi^L = \frac{RT}{z_j \mathcal{F}} \ln \frac{X_j^L}{X_j^S} - \frac{\Delta\mu_j^\circ}{z_j \mathcal{F}}. \quad (17)$$

These equations describe the relationship between the potential difference and the concentration of each component in the two phases. Normally in electrochemistry, the electrode is considered to be pure metal and the equations are

only applied to the species involved in electron transfer. Evaluated in this situation, Eq. (17) is equivalent to the Nernst equation (1).

From Eq. (17), we see that the standard chemical potential difference between the electrode and electrolyte $\Delta\mu_j^\circ$ can be broken into two terms

$$\Delta\mu_j^\circ = RT \ln \frac{X_j^{L,\text{Ref}}}{X_j^{S,\text{Ref}}} - z_j \mathcal{F} \Delta\psi^{\text{Ref}}. \quad (18)$$

$\Delta\psi^{\text{Ref}} = (\psi^S - \psi^L)^{\text{Ref}}$ and superscript Ref denotes the reference state for the standard potentials. The chosen value of the parameter $\Delta\psi^{\text{Ref}}$ can be shown to have a direct relationship with the surface energy of the electrochemical interface, the charge on the metal, and the deviation of the interface from the point of zero charge. As such, it is a materials parameter that is fixed for each metal/electrolyte system, even as the actual concentrations are changed. $\Delta\psi^{\text{Ref}}$ is equivalent to the ‘‘Galvani’’ potential of the electrode-electrolyte interface, and is related to the difference between the work functions of the electrode and electrolyte.

We choose as our reference state a metallic copper electrode in contact with a 1 mol/L CuSO_4 aqueous electrolyte, as described in Table 1. In order to perform equilibrium numerical simulations, some trace of H_2O and SO_4^{-2} must be permitted in the electrode and some trace of e^- must be permitted in the electrolyte. We arbitrarily choose a mole fraction of 10^{-6} for these trace components in the reference state. The remaining parameters are $W_{e^-} = 0$ J/mol, all other $W_j = 3.6 \times 10^5$ J/mol, $\kappa_\varphi = 3.6 \times 10^{-11}$ J/m, $\bar{V}_s = 1.8 \times 10^{-5}$ m³/mol, and $\epsilon = 6.95 \times 10^{-10}$ F/m.

Fixing the reference concentrations, we can examine the consequences of varying the potential difference around $\Delta\psi^{\text{Ref}}$. We simultaneously solve Eq. (17) for all four components, subject to charge neutrality and $\sum^N X_j = 1$ in each phase. The resulting mole fractions of the electrode and electrolyte are shown in Figure 3. We can see that, over the entire range of $\Delta\psi^{\text{Ref}}$, the electrode remains copper metal, with trace amounts of H_2O and SO_4^{-2} . Over most of

Table 1

Values of reference concentrations.

	$X_j^{L,\text{Ref}}$	$C_j^{L,\text{Ref}} / (\text{mol}/\text{m}^3)$	$X_j^{S,\text{Ref}}$	$C_j^{S,\text{Ref}} / (\text{mol}/\text{m}^3)$
Cu^{+2}	0.0180	1000	0.333	55600
SO_4^{-2}	0.0180	1000	1.0×10^{-6}	0.167
e^-	1.0×10^{-6}	0.0556	0.667	111000
H_2O	0.964	53600	9.99×10^{-7}	0.167

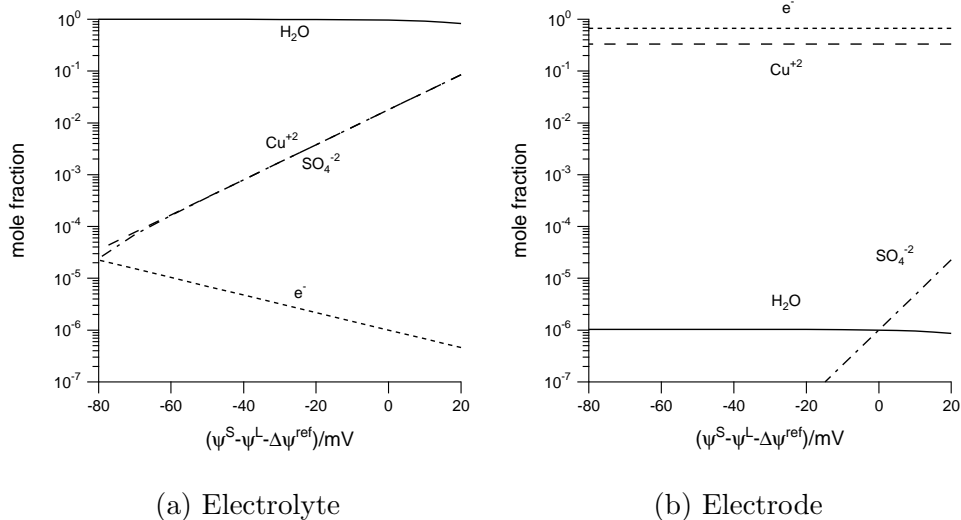


Fig. 3. Mole fraction as a function of applied potential for the electrode-electrolyte equilibrium. Note that the slope of SO_4^{-2} in the electrode is twice that in the electrolyte.

the displayed range, the electrolyte is predominantly water, with Cu^{+2} and SO_4^{-2} obeying Nernstian behavior.

The behavior of the trace amount of SO_4^{-2} in the electrode warrants discussion. If we assume the SO_4^{-2} concentration of the electrode is fixed, the Nernst relationship for SO_4^{-2} indicates that its concentration in the electrolyte should move in the opposite direction from Cu^{+2} in the electrolyte, for a given change in $\psi^S - \psi^L$, because of the sign change on z_j . The requirement of bulk charge neutrality in the electrolyte prevents this from occurring, however. If the concentration of Cu^{+2} in the electrolyte increases by an order of magnitude, charge neutrality requires that the concentration of SO_4^{-2} in the electrolyte increases by the same amount (neglecting e^-). In order for Eq. (17) to be satisfied for both Cu^{+2} and SO_4^{-2} , *i.e.*, for all species to be in electrochemical equilibrium, the concentration of SO_4^{-2} in the electrode must then increase by *two* orders of magnitude.

Another way to see the equilibrium relationship between these phases is on the quaternary phase diagram in Figure 4. The vertices of the diagram are pure Cu^{+2} , SO_4^{-2} , H_2O , and e^- . The plane shows the zero charge combinations and the tie lines between liquid and solid phases show the equilibria varying between $\text{Cu}(\text{M})\text{-H}_2\text{O}$ at negative electrode potentials and $\text{Cu}(\text{M})\text{-CuSO}_4$ at positive electrode potentials.

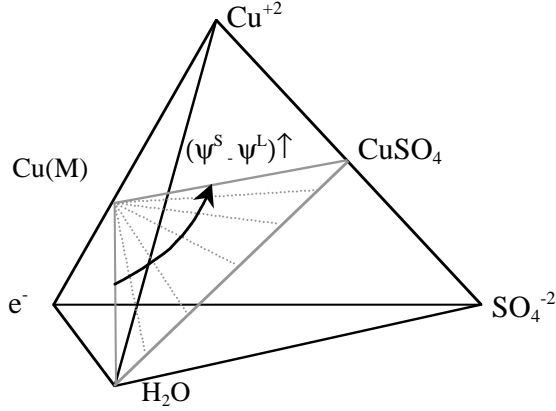


Fig. 4. Phase diagram and charge-neutral plane for Cu(M)–CuSO₄–H₂O.

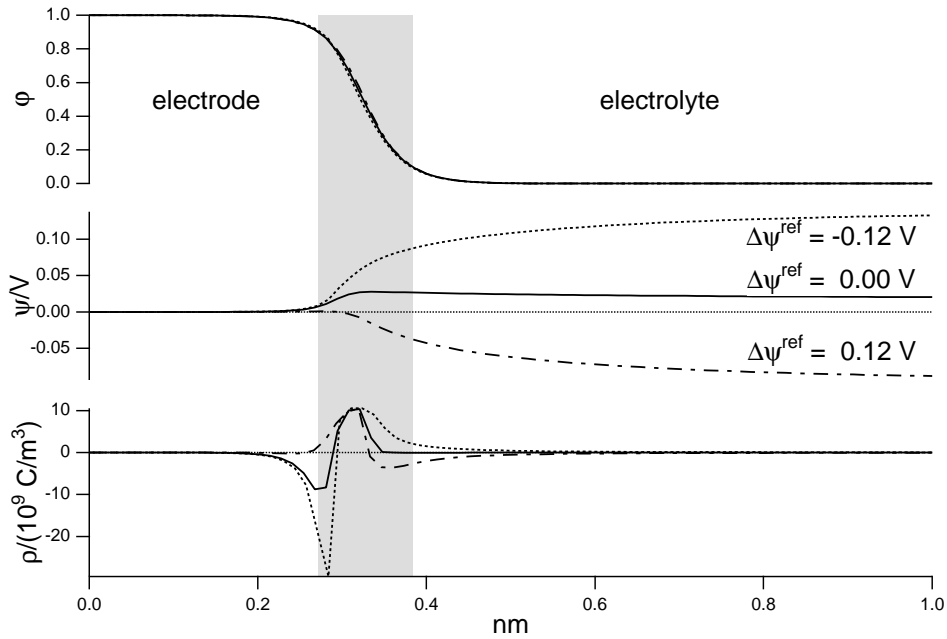


Fig. 5. Profiles through the 1D equilibrium interface for different values of $\Delta\psi^{\text{Ref}}$. The shaded area denotes the interfacial region $0.1 < \varphi < 0.9$.

2.6 Equilibrium profiles

Eqs. (3), (10), and (11) are solved with finite difference techniques (to second order in space) on a uniform grid. The sharp, two-phase initial condition was allowed to relax to equilibrium. The numerical methods are discussed in detail in Ref. [7]. The 1D interface between electrode and electrolyte is shown in Figures 5 and 6. The different curves are for fixed concentration and different values of $\Delta\psi^{\text{Ref}}$. We see that, as one might expect, the phase field φ is not particularly sensitive to $\Delta\psi^{\text{Ref}}$, but the charge distribution ρ is. All of the φ curves fall within 2% of a hyperbolic tangent profile, but the charge density

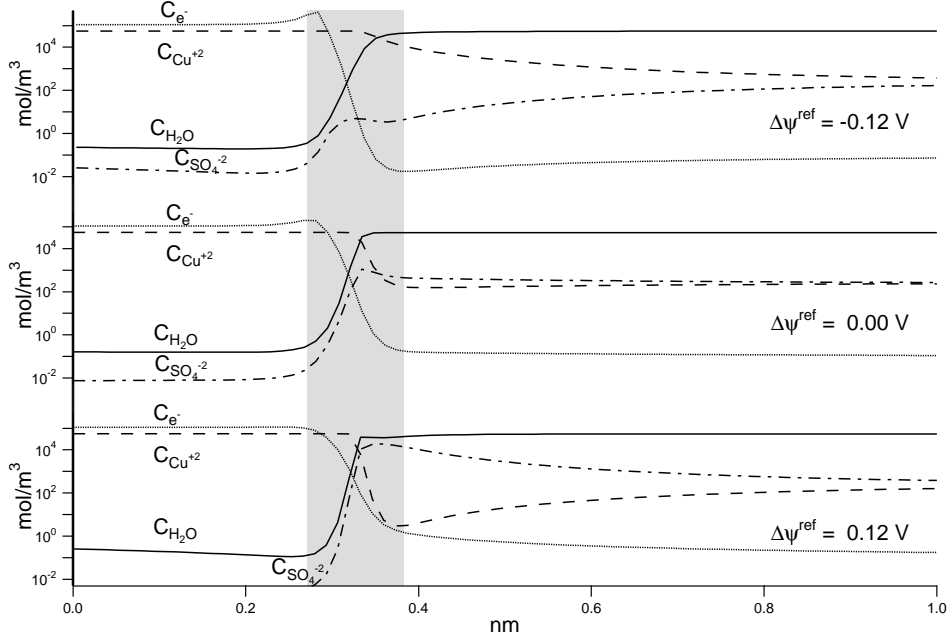


Fig. 6. Concentration profiles through the 1D equilibrium interface for different values of $\Delta\psi^{\text{Ref}}$. The shaded area denotes the interfacial region $0.1 < \varphi < 0.9$.

changes from a negatively charged electrode at $\Delta\psi^{\text{Ref}} = -0.12$ V to a positively charged electrode at $\Delta\psi^{\text{Ref}} = +0.12$ V. At $\Delta\psi^{\text{Ref}} = 0$ V, we see that there is essentially zero charge in the electrolyte, and the dipole charge in the electrode likewise sums to a very small charge (note that a dipole layer does not necessarily imply the presence of polar molecules [6]).

The charge distributions in Figure 5 are a result of the ionic distributions in Figure 6. At $\Delta\psi^{\text{Ref}} = -0.12$ V, there is a surplus of e^- at the electrode interface. Cu^{+2} remains at essentially the electrode density to some distance into the electrolyte, indicating an adsorbed layer of Cu^{+2} (note the specific adsorption of SO_4^{-2} in each case).

We examine the electrostatic potential profiles of Figure 5 in Figure 7. We fit each of the curves to $\psi = \psi_\infty + (\psi_0 - \psi_\infty) \exp(-x/l_\psi)$ and find excellent agreement for the decay length with $l_\psi = 0.304$ nm predicted by the Gouy-Chapman model. The deviation between fit and model at the left edge of the plot are because the Gouy-Chapman model assumes an abrupt electrode-electrolyte interface and the phase field model treats it as diffuse.

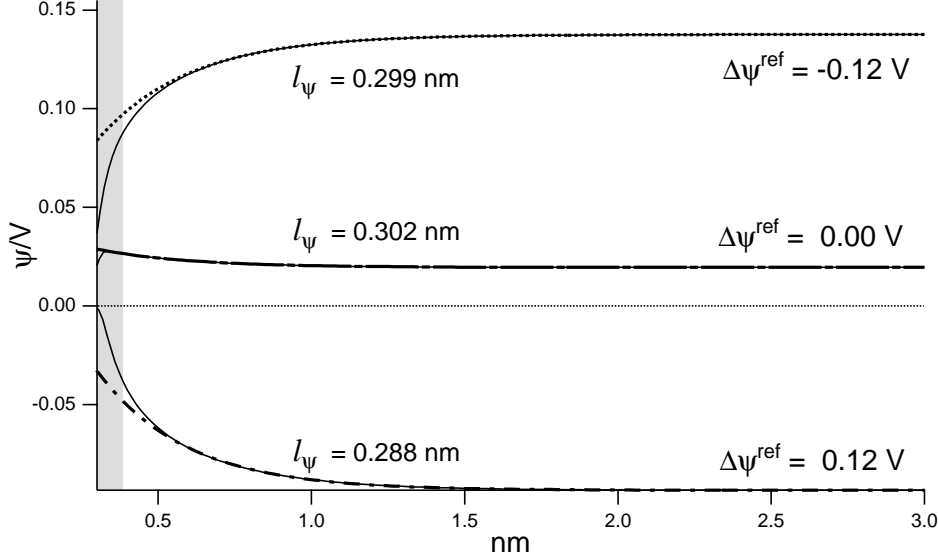


Fig. 7. Comparison of electrostatic potential profiles (light solid lines) with predictions of Gouy-Chapman model (heavy dashed lines). The shaded area denotes the interfacial region $0.1 < \varphi < 0.9$.

2.7 Interface properties

From a 1D analysis of Eq. (9), the equilibrium surface energy is described by

$$\gamma = \int_{-\infty}^{\infty} [\kappa_{\varphi} (\varphi')^2 - \epsilon (\psi')^2] dx \quad (19)$$

where the prime denotes the derivative with respect to position. The surface charge on the electrode is related to the surface energy by

$$-\frac{\partial \gamma}{\partial \Delta \psi^{\text{Ref}}} = \sigma^S \equiv \int_{-\infty}^{\infty} p(\varphi) \rho dx \quad (20)$$

(this is identical with the sharp-interface prediction of Eq. (6)).

We plot the surface energy, calculated with Eq. (19), for different values of $\Delta \psi^{\text{Ref}}$ in Figure 8. These curves are quite similar to the “electrocapillary” curves of surface energy measured on mercury electrodes [6] for different applied potentials. In the electrocapillary experiment, the applied potential is varied at an inert electrode with a fixed Galvani potential. In our simulations, the Galvani potential is varied at a chemically reactive, but unbiased, interface. For each curve, there is a value of $\Delta \psi^{\text{Ref}}$ for which the surface energy is a maximum. We see from Figure 9, which is calculated from either side of Eq. (20), that there is a maximum surface energy at the “potential of zero charge”, just as is predicted by the Gouy-Chapman model.

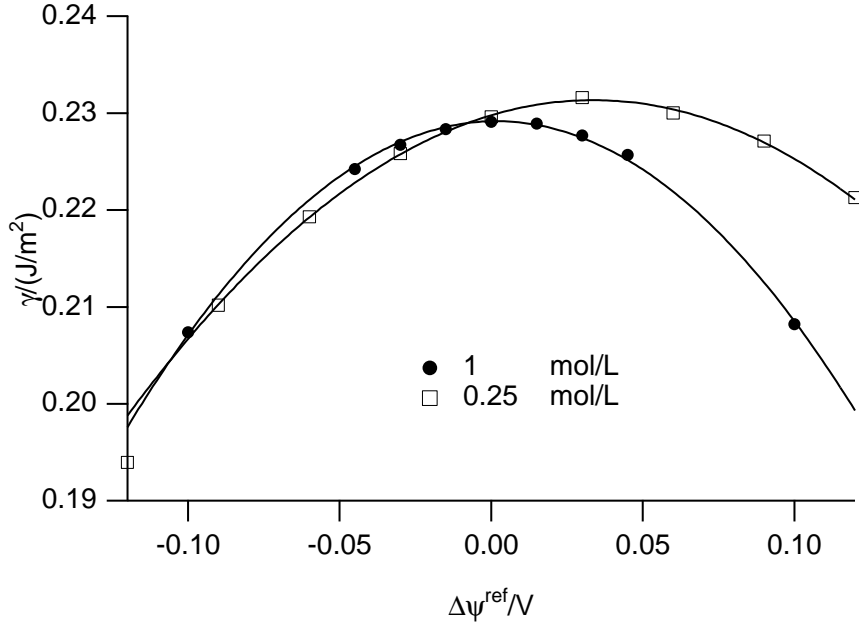


Fig. 8. Surface energy as a function of $\Delta\psi^{\text{Ref}}$. The lines are to guide the eye.

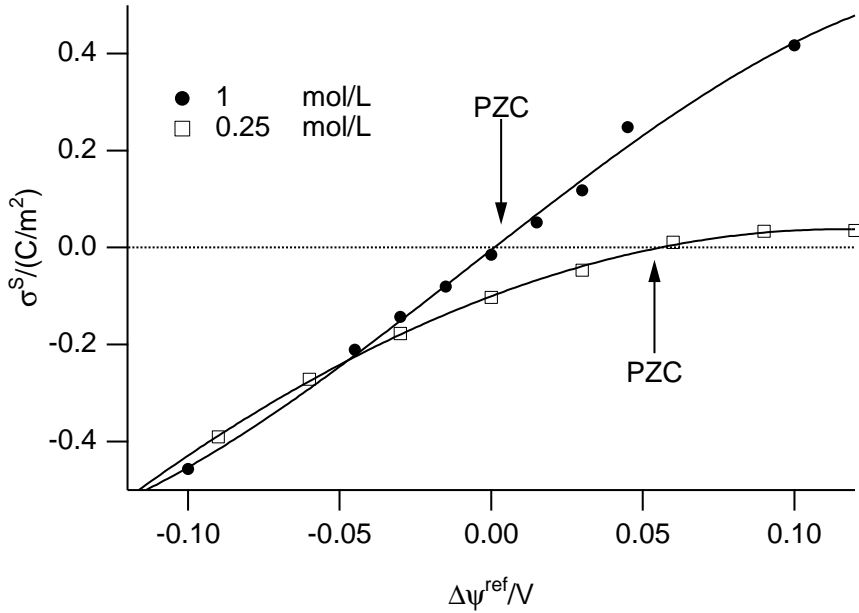


Fig. 9. Electrode surface charge as a function of $\Delta\psi^{\text{Ref}}$. The lines are to guide the eye.

3 Conclusions

- Phase field model of electrochemical interface exhibits double layer behavior.
- Decay length of electrostatic potential are consistent with sharp-interface models.
- Dependence of surface energy (“electrocapillary curves”) and surface charge on potential are consistent with sharp-interface models.

- Crucial presence of charged species in electrochemistry leads to rich interactions between concentration, electrostatic potential, and phase stability.
- Dynamic treatments of this model arise naturally [7].

4 Acknowledgements

We are grateful for many fruitful discussions with Ugo Bertocci, Gery Stafford, Tom Moffat, Daniel Josell, Daniel Wheeler, John Cahn, Sam Coriell, and Alex Lobkovsky.

References

- [1] W. J. Boettinger, J. A. Warren, Simulation of the cell to plane front transition during directional solidification at high velocity, *J. Cryst. Growth* 200 (1999) 583–591.
- [2] F. Drolet, K. R. Elder, M. Grant, J. M. Kosterlitz, Phase-field modeling of eutectic growth, *Phys. Rev. E* 61 (6) (2000) 6705–6720.
- [3] P. C. Andricacos, C. Uzoh, J. O. Dukovic, J. Horkans, H. Deligianni, Damascene copper electroplating for chip interconnections, *IBM J. Res. Develop.* 42 (5) (1998) 567–574.
- [4] D. Josell, D. Wheeler, W. H. Huber, T. P. Moffat, Superconformal electrodeposition in submicron features, *Phys. Rev. Lett.* 87 (1).
- [5] A. J. Bard, L. R. Faulkner, *Electrochemical Methods: Fundamentals and Applications*, John Wiley & Sons, Inc., New York, 2001.
- [6] D. C. Grahame, The electrical double layer and the theory of electrocapillarity, *Chem. Rev.* 41 (1947) 441–501.
- [7] J. E. Guyer, W. J. Boettinger, J. A. Warren, G. B. McFadden, Phase-field modeling of electrochemistry, unpublished research.